Universality and Lepton Flavor Violation in Υ Decays at CLEO

J.E. Duboscq[a], for the CLEO Collaboration *

[a]Wilson Laboratory, Cornell University, Ithaca, NY, 14853, USA

I present two analyses done with the CLEOIII detector at CESR. The first is a search for the LFV decay $\Upsilon \to \mu\tau$ with preliminary results, and the second constrains Lepton Universality in $\Upsilon \to \tau\tau$ relative to $\Upsilon \to \mu\mu$. This second analysis, whose results are final, has dramatically improved uncertainties relative to other such measurements, and is also the first observation of the decay $\Upsilon(3S) \to \tau\tau$. A limit is also set on the involvement of a CP odd Higgs in the decay of the $\Upsilon(1S)$ to τ pairs.

1. Introduction

In this report, I present results on two analyses done with data taken using the CLEOIII detector on the CESR storage ring by the CLEO Collaboration. The first analysis is a search for the Lepton Flavor Violating (LFV) decay $\Upsilon(nS) \to \mu\tau$, $n = 1, 2, 3$ - all results from this analysis are preliminary. The second analysis tests Lepton Universality in the decays $\Upsilon \to \mu\mu, \tau\tau$, $n = 1, 2, 3$ - all results from this analysis are final.

The CLEOIII detector is a modern almost hermetic detector, sitting on the CESR beamline, where positrons and electrons collide with an energy $\approx 5\,\text{GeV}$. The detector included a silicon strip detector at its center, surrounded by a wire chamber, which provided tracking and dE/dx information, a Cesium Iodide calorimeter, and a Ring Imaging Cerenkov Detector all in a 1.5 Tesla magnetic field. Outside of this were a series of muon chambers. Further details of the detector can be found in [1].

The data used in this analysis comprise the $\Upsilon(nS)$, $n = 1, 2, 3$ datasets, along with a portion of the $\Upsilon(4S)$ data for validation purposes. These datasets include data taken at the peaks of the resonances, as well as smaller datasets taken some $30 - 40$MeV below the resonances. The total sample includes approximately 20×10^6 $\Upsilon(1S)$, 10×10^6 $\Upsilon(2S)$ and 5×10^6 $\Upsilon(3S)$ decays.

*I would like to thank A.Lusiani and the staff of Tau06 for a wonderfully stimulating conference.

2. Search for LFV in $\Upsilon \to \mu\tau$

Lepton Flavor Violation (LFV) might provide a key to understanding Lepton Number Violation, as well as Baryon Number Violation, and hence might be helpful in understanding the matter/anti-matter asymmetry in the Universe. LFV decays in the Υ sector can be related to LFV decays of the τ lepton by a simple reordering of input and output lines in the Feynman diagram for the process $e^+e^- \to \gamma* \to \Upsilon* \to \tau\mu$. In this way, [2] have show that a result of $B(\tau \to 3\mu) < 10^{-6}$ implies that $B(\Upsilon \to \mu\tau) < 10^{-2}$.

LFV decays of the Υ to lepton pairs might also be expected in the presence of SUSY loops [3], or other exotic physics such as leptoquarks and theories with more than one Z boson.

A general ansatz for talking about LFV decays of the Υ involves a generic four fermion interaction vertex between two b quarks, a muon and a τ. With the coupling constant at the interaction denoted α_N and the relevant new physics mass scale denoted Λ, one finds [4]:

$$\frac{B(\Upsilon \to \mu\tau)}{B(\Upsilon \to \tau\tau)} \propto (\alpha_N/\alpha)^2 (M_\Upsilon/\Lambda)^4$$

.

The CLEO analysis presented here is a search for $\Upsilon(nS) \to \mu\tau$, $\tau \to e\nu\nu$, n=1,2,3. The final observed state is a two track event with a muon and a electron and missing energy. The muon would have an energy a little below the beam energy, while the electron energy spectrum would be approximately that expected for electrons in normal τ pair events.

The fit to the data is performed using an extended maximum likelihood function, composed of a product PDF, summed over expect signal LFV shapes, direct $ee \to \tau\tau$ shapes, $ee \to \mu\mu\gamma$ and $ee \to \mu\mu$ with $\mu \to e\nu\nu$ decays. Data from the $\Upsilon(4S)$ resonance, and off resonance data are used as calibration and control samples.

Fig 1 shows the beam energy scaled electron momentum spectrum versus the scaled muon momentum spectrum, in $\Upsilon(4S)$ data where no signal is expected, since even $\Upsilon(4S) \to \tau\tau$ is too small to be observed.

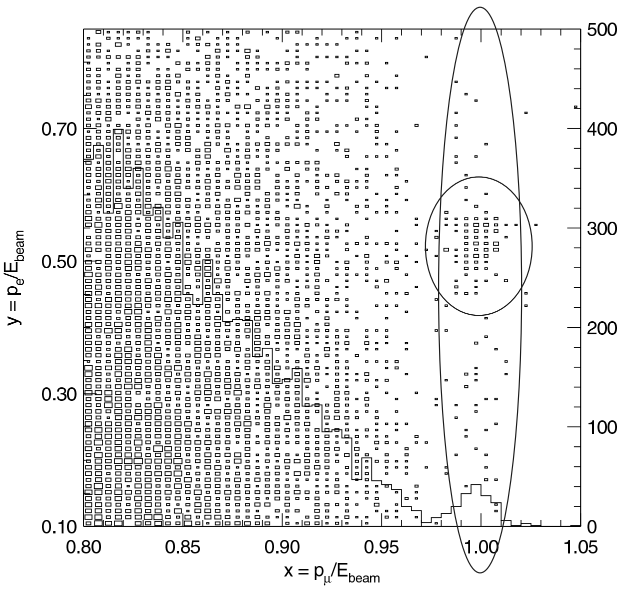

Figure 1. Beam energy scaled electron versus the scaled muon momentum in $\Upsilon(4S)$ data. The left hand side is dominated by τ pair decays. The signal region is a vertical strip near $p_\mu/E_{Beam} \approx 0.97$. The concentration of events near $p_\mu/E_{Beam} = 1$ and $p_e/E_{Beam} = 0.5$ is from $\mu\mu\gamma$ backgrounds. Also at $p_\mu/E_{Beam} = 1$ are events from muon decays to electrons in $\mu\mu$ production.

Fig 2 shows the data distributions for the fit quantities at the $\Upsilon(1S)$. Note the clear absence of a signal, especially in the muon momentum spectrum.

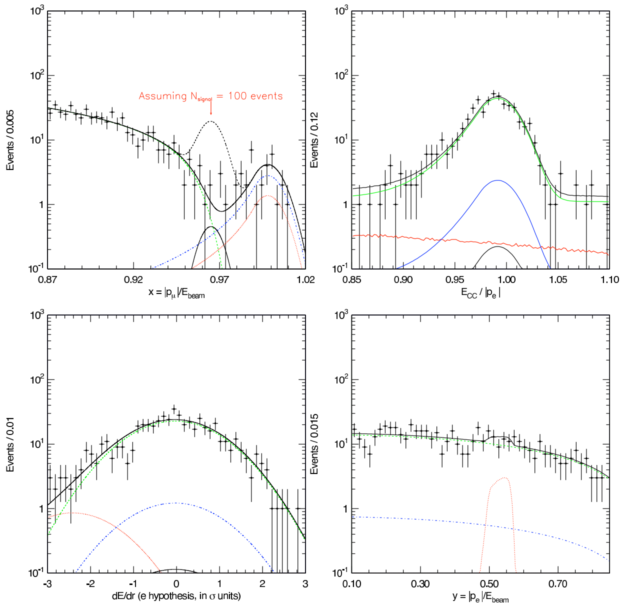

Figure 2. Likelihood distributions for the scaled muon momentum, E/p, dE/dx and scaled momentum for the electron candidate. Note the curve indicating what 100 signal events would look like.

Preliminary analysis results are summarized in Table 1. The largest systematic uncertainties are from PDF shapes and their correlations. This study represents the first limits on $B(\Upsilon \to \tau\mu)$. These limits set a lower limit of ≈ 1 TeV on the scale of new physics, assuming a strong coupling.

3. Lepton Universality in $\Upsilon \to \mu\mu, \tau\tau$

In the Standard Model, the couplings between leptons and gauge bosons are independent of the lepton flavor, so the branching fractions for the decay $\Upsilon(nS) \to l^+l^-$ should be independent of the flavor of the lepton l, except for negligible final state lepton mass effects. Any deviation from

Resonance	$\Upsilon(1S)$	$\Upsilon(2S)$	$\Upsilon(3S)$
Efficiency	8.9%	8.9%	8.9%
Events	< 10.0	< 10.7	< 8.5
$B(\Upsilon \to \tau\mu)$ (10^{-6})	< 6.2	< 25	< 22
$B(\tau\mu)/B(\mu\mu)$	$< 0.023\%$	$< 0.17\%$	$< 0.13\%$

Table 1
Preliminary results for the LFV search. Displayed are the signal MC efficiencies, raw event counts, resulting branching fractions, and the ratio $B(\Upsilon \to \tau\mu)/B(\Upsilon \to \mu\mu)$. All limits are 90% confidence level upper limits.

unity for the ratio of branching fractions $\mathcal{R}^{\Upsilon}_{\tau\tau} = B(\Upsilon(nS) \to \tau\tau)/B(\Upsilon(nS) \to \mu\mu)$ would indicate the presence of new physics. The ratio $\mathcal{R}^{\Upsilon}_{\tau\tau}$ is sensitive to the mechanism proposed in [5], in which a low mass CP-odd Higgs boson, A^0, mediates the decay chain $\Upsilon(1S) \to \eta_b\gamma, \eta_b \to A^0 \to \tau\tau$.

CLEO has recently measured the partial width, Γ_{ee}, from $e^+e^- \to \Upsilon(nS)$ [6], $n = 1, 2, 3$, as well as the branching fraction for $\Upsilon(nS) \to \mu^+\mu^-$ [7]. This analysis complements these measurements by measuring $\mathcal{R}^{\Upsilon}_{\tau\tau}$ directly, and scales this result to obtain $B(\Upsilon(nS) \to \tau\tau)$. An upper limit on the product branching fraction $B(\Upsilon(1S) \to \eta_b\gamma)B(\eta_b \to A^0 \to \tau\tau)$ is extracted.

The analysis technique, similar to that in [7], isolates the $\Upsilon \to \mu\mu, \tau\tau$ signals by subtracting a luminosity and beam energy weighted number of events observed in off-resonance data from the number observed in on-resonance data, and, after further background correction, attributes the remaining signal to Υ decays to leptons. Selection criteria are developed to isolate $\mu\mu$ and $\tau\tau$ final states using a subset of the data acquired near the $\Upsilon(4S)$. Another subset of $\Upsilon(4S)$ data is used to verify that subtracting the scaled off-resonance data from the on-resonance data produces no signal for $\Upsilon(4S) \to \tau\tau, \mu\mu$, indicating that non-$\Upsilon$ backgrounds are suppressed by the subtraction. As a further crosscheck, the off-resonance production cross-sections for $\tau\tau$ and $\mu\mu$ are verified to agree with theoretical expectations.

The final states chosen for both the $\Upsilon \to \mu\mu$ and $\Upsilon \to \tau\tau$ decays are required to have exactly two good quality charged tracks of opposite charge.

Selection criteria for the $\mu\mu$ final state closely parallel those of [7], requiring tracks with momenta scaled to $E_{\rm beam}$ between 0.7 and 1.15, of which at least one is positively identified as a muon. The energy deposited by a particle in a calorimeter shower, $E_{\rm CC}$, is required to satisfy $100\,{\rm MeV} < E_{\rm CC} < 600\,{\rm MeV}$. No more than one shower unassociated with a track and with energy above 1% of $E_{\rm beam}$ is allowed.

At least two neutrinos from final states of $e^+e^- \to \tau\tau$ escape detection. Thanks to CLEO-III's hermeticity, the following criteria select such events despite the energy carried away by the unreconstructed neutrinos. The total charged track momentum transverse to the beam direction must be greater than 10% of $E_{\rm beam}$, and the total charged track momentum must point into the barrel region of the detector where tracking and calorimetry are optimal. Events with collinear tracks are eliminated. Tracks are required to have momenta greater than 10% of $E_{\rm beam}$ to ensure that they are well-reconstructed, and, to minimize pollution from two-particle final states, they are required to have momenta less than 90% of $E_{\rm beam}$. The total observed energy due to charged and neutral particles in the calorimeter is similarly required to be between 20% and 90% of the total center-of-mass energy. To reduce overlap confusion between neutral and charged particles, a shower's energy scaled to its associated track's momentum must be less than 1.1.

Final states are further exclusively divided according to the results of particle identification into (e, e), (μ, e), (e, μ), (μ, μ), (e, X), (μ, X), (X, X) sub-samples, with particles listed in descending momentum order. The first (second) particle listed is referred to as the tag (signal). The sub-samples are used to crosscheck consistency of results across decay modes. Lepton identification requires a track momentum greater than 500 MeV to ensure that the track intersects the calorimeter. Electrons are identified by requiring that $0.85 < E_{\rm CC}/P < 1.10$, where P is the track momentum, and that the specific ionization along the track's path in the drift chamber be consistent with the expectation for an electron. A muon candidate in τ decays is a charged track which is not identified as an electron, having momentum above 2 GeV (1.5 GeV) for a tag (signal) track and confined to the central barrel where beam related background is a minimum. Furthermore, the energy deposited in the calorimeter for this track must be between 100 and 600 MeV, and the particle must penetrate at least three interaction lengths into the muon detector. Particles identified as neither e nor μ are designated X, and are a mixture of hadrons and unidentified leptons.

The decay products of τ pairs from Υ decays tend to be separated into distinct hemispheres. Since the photon spectrum expected in τ decays depends on the identity of the charged particle, calorimeter showers are assigned to either the tag or signal hemisphere according to their proximity to the tag side track direction. For each τ decay mode pair, the number of unmatched showers in the calorimeter as well as the total energy of these showers on each side of the decay are used as selection criteria.

For the (e, e) and (μ, μ) modes, the sum of the magnitudes of the tag and signal track momenta must be less than $1.5E_{\rm beam}$, reducing the contamination from radiative dilepton events. To reduce backgrounds from $e^+e^- \to l^+l^-\gamma\gamma$ and $e^+e^- \to e^+e^-l^+l^-$ in the (e, e), (μ, μ), (X, X) categories, the minimum polar angle of any unseen particles, deduced from energy-momentum conservation, is required to point into the barrel region, where calorimetry cuts will ensure rejection.

Potential backgrounds due to cosmic rays are accounted for as in [7]. In all cases these were negligible.

Figure 3 shows the superimposed on-resonance

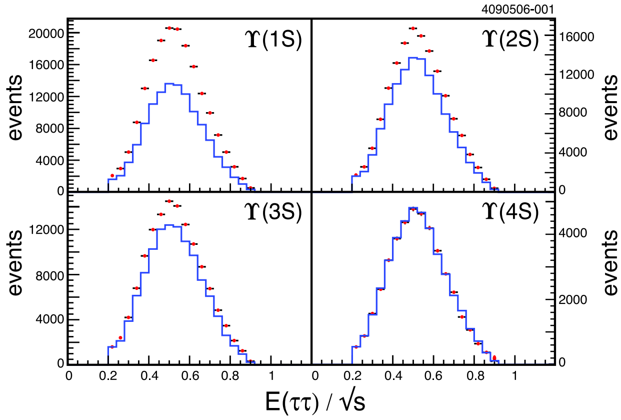

Figure 3. Total energy distributions, scaled to center of mass energy, $E_{\tau\tau}/\sqrt{s}$ for the $\tau\tau$ final states at the $\Upsilon(nS), n = 1, 2, 3, 4$ on (points) and scaled off (histograms) resonance. The excess of on-resonance relative to scaled off-resonance data is attributed to Υ decays for the lower resonances, while the agreement at the $\Upsilon(4S)$ tests the validity of the subtraction.

and scaled off-resonance total energy distributions for the $\tau\tau$ sample for all resonances. The scale factor is $S = (\mathcal{L}_{\rm On}/\mathcal{L}_{\rm Off})(s_{\rm Off}/s_{\rm On})\delta_{\rm interf}$, where $\mathcal{L}$ and s are the data luminosity and squared center of mass collision energies on and off the resonances, and $\delta_{\rm interf}$ is an interference correction. The luminosity is derived from the process $e^+e^- \to \gamma\gamma$ [8], which does not suffer backgrounds from direct Υ decays. The interference correction $\delta_{\rm interf}$ accounts for the small interference between the process $e^+e^- \to ll$ and $e^+e^- \to \Upsilon \to ll$ and is estimated [7] to be 0.984 (0.961, 0.982) at the $\Upsilon(1S)$ $(2S, 3S)$ and negligible for the $\Upsilon(4S)$. Note that the interference largely cancels in the ratios considered in this work. The agreement of the distributions for the $\Upsilon(4S)$ validates the subtraction technique, and also highlights the absence of any process whose cross-section does not vary as $1/s$. This agreement extends to the individual sub-samples.

The ratio of measured relative lepton pair production cross-sections, $\mathcal{R}^{\rm Off}_{\tau\tau} = \sigma_{\tau\tau}/\sigma_{\mu\mu}$, with respect to that theoretically expected at the off-resonance points, $\mathcal{R}_{\tau\tau}^{\rm Off\ theory} = \sigma_{\tau\tau}^{\rm theory}/\sigma_{\mu\mu}^{\rm theory}$ is $\mathcal{R}_{\tau\tau}^{\rm Off}/\mathcal{R}_{\tau\tau}^{\rm Off\ theory} = 0.96 \pm 0.03$ (0.97 ± 0.03, 0.97 ± 0.03 , 1.00 ± 0.03) below the $\Upsilon(1S)$ ($2S$, $3S$, $4S$) for the sum of all τ decay mode pairs, with statistical and systematic uncertainties added in quadrature. The expectation $\mathcal{R}_{\tau\tau}^{\rm Off\ theory} = 0.83 \pm 0.02\,({\rm syst})$ [2], which is found to be numerically independent of the particular resonance considered, and the reconstruction efficiencies are derived from the FPair [9] and Koralb/Tauola [11–13] Monte Carlos. Backgrounds were corrected by using $e^+e^- \to q\overline{q}(q = u, d, c, s)$ Monte Carlo simulations [16] [15] [13] [14]. The scatter in the central values of $\mathcal{R}_{\tau\tau}^{\rm Off}/\mathcal{R}_{\tau\tau}^{\rm Off\ theory}$ indicates that systematic uncertainties are small.

The reconstruction efficiency for observing $\Upsilon \to \mu\mu$ is derived from the CLEO GEANT-based simulation [16] [15] [13] [14], as shown in Table 2. This efficiency is found to be constant across the resonances.

The reconstruction efficiency for observing $\Upsilon \to \tau\tau$ is derived using the Koralb/Tauola event generator integrated into the Monte Carlo simulation. Although this generator models the process $e^+e^- \to \gamma^* \to \tau^+\tau^-$, the quantum numbers of the Υ and γ are the same so it can be used as long as initial state radiation (ISR) effects are not included. This efficiency is also found to be consistent across all resonances within any given $\tau\tau$ decay channel.

Results of the subtraction are summarized in Table 2, showing the first observation of $\Upsilon(3S) \to \tau\tau$.

Backgrounds resulting from cascade decays within the $b\overline{b}$ system to ll are estimated using the Monte Carlo simulation, with branching fractions scaled to the values measured in this study. Cascade backgrounds with non $\mu\mu$ and non $\tau\tau$ final states are estimated directly from the Monte Carlo simulation.

Figure 4 displays the off-resonance subtracted data, superimposed on Monte Carlo expectations. The distributions shown are a sampling of τ decay modes for the momenta of the signal and tag tracks, as well as the total reconstructed energy. In all cases the Monte Carlo expectations are consistent with the data assuming lepton universality and branching fractions as measured in [7]. The agreement across the various kinematic quantities indicates that backgrounds are well controlled.

Figure 5 shows the agreement across all $\tau\tau$ sub-samples of the ratio of off-resonance cross sections for $\tau\tau$ and $\mu\mu$ production, relative to expectation, as well as the ratio of branching fractions for each of these decay modes at the different Υ resonances. The agreement across $\tau\tau$ sub-samples both on and off the resonances is again an indication that backgrounds are small and well estimated.

The ratio of branching fractions and final branching fractions are listed in Table 3. These results show that lepton universality is respected in Υ decay within the $\approx 10\%$ measurement uncertainties.

Systematic uncertainties, summarized in Table 4, are estimated for the ratio of branching fractions, and for the absolute branching fraction. The ratio of branching fractions is insensitive to some common systematic uncertainties. For instance, the uncertainty on $\mathcal{R}_{\tau\tau}^{\Upsilon}$ due to a conservative 1% variation in the scale factor S, as determined using the process $e^+e^- \to \mu\mu$ near the $\Upsilon(4S)$ resonance, is found to be 0.4% or less.

Most systematic uncertainties due specifically to ll selection are derived by a variation of the selection criteria over reasonable ranges in the $\Upsilon(1S)$ sample, which has the lowest energy released in its decay. The most significant of these are due to momentum selection (1.3%), calorimeter energy selection (1.1%) and angular selection (1.1%). The systematic uncertainty due to modeling of the trigger, also included in the ll selection, is estimated by using a loose pre-scaled tracking trigger and comparing it to the more sophisticated triggers used in this analysis. This variation leads to a systematic uncertainty estimate of 1.6%.

Backgrounds are assumed to be due solely to Υ decays. As in [7], these were chiefly due to cascade decays to lower resonances, and are estimated to be 2.5% (15%, 11%) of the $\tau\tau$ sample at

[2]This expectation is lower than 1 because of the larger phase space available for initial state radiation production of $\mu\mu$ relative to $\tau\tau$ final states.

	$\Upsilon(1S)$	$\Upsilon(2S)$	$\Upsilon(3S)$
$\tilde{N}(\mu\mu)$ (10^3)	345 ± 7	121 ± 7	82 ± 7
$\epsilon(\mu\mu)$ (%)	65.4 ± 1.2	65.0 ± 1.1	65.1 ± 1.2
$N(\Upsilon \to \mu\mu)$ (10^3)	527 ± 15	185 ± 11	126 ± 11
$\tilde{N}(\tau\tau)$ (10^3)	60.1 ± 1.5	21.8 ± 1.5	14.8 ± 1.5
$\epsilon(\tau\tau)$ (%)	11.2 ± 0.1	11.3 ± 0.1	11.1 ± 0.1
$N(\Upsilon \to \tau\tau)$ (10^3)	537 ± 14	193 ± 12	132 ± 13

Table 2
Summary of reconstructed events for $\Upsilon \to \mu\mu$ (top) and $\Upsilon \to \tau\tau$ (bottom). Shown are the number of events ($\tilde{N}_{ll}$) after subtraction of backgrounds estimated from scaled off-resonance data and Υ feed-through estimated from the Monte Carlo simulation, the signal efficiency ($\epsilon(ll)$), and the total efficiency corrected number of signal events $N(\Upsilon \to ll) = \tilde{N}_{ll}/\epsilon(ll)$. The $\tau\tau$ events are summed over all decay modes of the τ. Uncertainties included in this table include data and Monte Carlo statistical uncertainties, uncertainties on backgrounds, and detector modeling (included only for $\epsilon(\mu\mu)$ to avoid double counting in the final ratio).

	$\mathcal{R}^{\Upsilon}_{\tau\tau}$	$B(\Upsilon \to \tau\tau\ )$ (%)
$\Upsilon(1S)$	$1.02 \pm 0.02 \pm 0.05$	$2.54 \pm 0.04 \pm 0.12$
$\Upsilon(2S)$	$1.04 \pm 0.04 \pm 0.05$	$2.11 \pm 0.07 \pm 0.13$
$\Upsilon(3S)$	$1.07 \pm 0.08 \pm 0.05$	$2.55 \pm 0.19 \pm 0.15$

Table 3
Final results on the ratio of branching fractions to $\tau\tau$ and $\mu\mu$ final states, and the absolute branching fraction for $\Upsilon \to \tau\tau$. Included are both statistical and systematic uncertainties, as detailed in the text.

the $\Upsilon(1S)(2S, 3S)$, with an estimated uncertainty contribution to $\mathcal{R}^{\Upsilon}_{\tau\tau}$ of 0.1% (2.4%, 1.3%).

The uncertainty due to detector modeling in [7] was estimated to be 1.7%: this value is used here conservatively for the systematic uncertainty on the ratio.

The modeling of the physics in $\Upsilon(1S) \to \mu\mu$, obtained by varying the decay model for $\Upsilon \to \mu\mu$ between the Monte Carlo simulation and Koralb with ISR simulation turned off, contributes an uncertainty 2%. This uncertainty is consistent with the variation in the product of the off-resonance cross section and reconstruction efficiency using the FPair, Koralb, and Babayaga Monte Carlo simulations, and is thus likely conservative, as direct $\mu\mu$ production from the Υ at the peak involves much lower energy final state photons than off resonance production. An uncorrelated uncertainty of 2% for modeling of $\Upsilon \to \tau\tau$ is assumed, consistent with the uncertainty on the off-resonance production cross section derived in previous analyses, and is again conservative as on-resonance production of $\tau\tau$ final states involves fewer photons than direct continuum production. To test the sensitivity to ISR simulation, the reconstruction efficiency for events with no ISR simulation is compared to that for events generated with ISR simulation turned on and re-weighted according to the relative value of the Υ line shape at the τ pair mass. These two efficiencies agree to within 0.8% of their central value.

The mechanism described in [5] could induce a value of $\mathcal{R}^{\Upsilon}_{\tau\tau}$ not equal to one. By assuming that the mass of the $\eta_b(1S)$ is $100\,\mathrm{MeV/c^2}$ below the $\Upsilon(1S)$ mass, consistent with the largest value in [17], the value quoted for $\mathcal{R}^{\Upsilon}_{\tau\tau}(1S)$ can be translated into an upper limit on the combined branching fraction of $B(\Upsilon(1S) \to \eta_b\gamma)B(\eta_b \to$

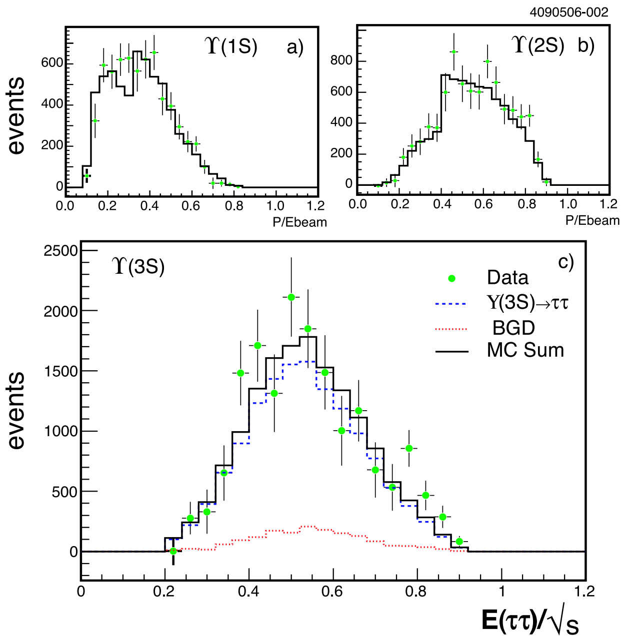

Figure 4. Distributions for the $\tau\tau$ final states at the $\Upsilon(nS), n = 1, 2, 3$ after subtraction of S-scaled off-resonance data. Distribution a) shows $P_{\mathrm{sig}}/E_{\mathrm{beam}}$ in $\Upsilon(1S)$ decays for the sum of τ decay modes including exactly two identified leptons. Distribution b) shows $P_{\mathrm{tag}}/E_{\mathrm{beam}}$ in $\Upsilon(2S)$ decays for the sum of τ decay modes including exactly one identified lepton. Distribution c) shows $E_{\tau\tau}/\sqrt{s}$ for $\Upsilon(3S)$ for the sum of all τ decay modes. In all cases, the solid line shows the expected total signal and background distributions, assuming lepton universality. In distribution c), the signal and total background distributions are explicitly displayed. Data uncertainties shown are purely statistical.

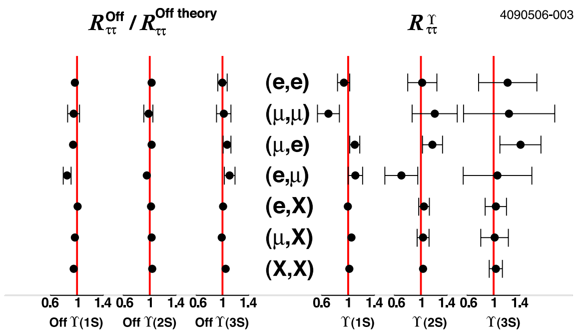

Figure 5. Breakdown by mode of off- and on-resonance data at the different resonances. On the left, the ratio of the production cross section for $e^+e^- \to ll(l = \tau, \mu)$, relative to its expectation, is plotted for data taken below the Υ for each τ decay mode pair. On the right, the ratio of branching fractions for the process $\Upsilon \to ll(l = \tau, \mu)$ is displayed. The line centered at 1 in each case represents the Standard Model expectation. Errors shown are statistical.

$A^0 \to \tau\tau) < 0.27\%$ at 95% confidence level. Since the transition photon is not explicitly reconstructed, this limit is valid for all η_b that approximately satisfy $M(\Upsilon(1S)) - M(\eta_b) + \Gamma(\eta_b)) < \mathcal{O}(100\,\mathrm{MeV}/c^2)$.

In summary, using the full sample of on-resonance $\Upsilon(nS)$, $n = 1, 2, 3$, collected at the CLEO-III detector, we have made the first observation of the decay $\Upsilon(3S) \to \tau\tau$. We have also reported the ratio of branching fractions of Υ decays to $\tau\tau$ and $\mu\mu$ final states, and find these to be consistent with expectations from the Standard Model. These ratios have been combined with results from [7] to provide absolute branching fractions for the process $\Upsilon \to \tau\tau$, shown in Table 3, resulting in the most precise single measurement of $B(\Upsilon(1S) \to \tau\tau)$ [18], a much improved value of $B(\Upsilon(2S) \to \tau\tau)$ and a first measurement of $B(\Upsilon(3S) \to \tau\tau)$. The ratio of branching fractions for $\tau\tau$ and $\mu\mu$ final states has also been used to set a limit on a possible Higgs mediated decay window.

Source	σ_{syst} (%)
S	0.2 / 0.4 / 0.3
Background	0.1 / 2.4 / 1.3
τ, μ Selection	2.9
$\Upsilon \to \mu\mu$ Model	2.0
$\Upsilon \to \tau\tau$ Model	2.0
Detector Model	1.7
MC Statistics	1.9 / 1.0 / 1.0
$\sigma(\mathcal{R}^{\Upsilon}_{\tau\tau})/\mathcal{R}^{\Upsilon}_{\tau\tau}$	4.8 / 4.4 / 4.6
$\sigma(B_{\tau\tau})/B_{\tau\tau}$	4.0 / 3.8 / 3.9

Table 4
Summary of systematic uncertainties. The entry $\sigma(\mathcal{R}^{\Upsilon}_{\tau\tau})/\mathcal{R}^{\Upsilon}_{\tau\tau}$ indicates the relative uncertainty on $\mathcal{R}^{\Upsilon}_{\tau\tau}$, while the $\sigma(B_{\tau\tau})/B_{\tau\tau}$ entry indicates uncertainties specific to τ decay modes used in addition to those in [7] to obtain $B(\Upsilon \to \tau\tau)$. The uncertainty on S and the background are included in the statistical uncertainty only. Lines with three entries indicate the contribution from the $\Upsilon(1S)$, $\Upsilon(2S)$ and $\Upsilon(3S)$, respectively.

We gratefully acknowledge the effort of the CESR staff in providing us with excellent luminosity and running conditions. We also thank M.A. Sanchis-Lozano for many illuminating discussions. This work was supported by the A.P. Sloan Foundation, the National Science Foundation, the U.S. Department of Energy, and the Natural Sciences and Engineering Research Council of Canada.

REFERENCES

1. G. Viehhauser, Nucl. Inst. Meth. A **462**, 146 (2001); D. Peterson *et al.*, Nucl. Inst. Meth. A **478**, 142 (2002); M. Artuso *et al.*, Nucl. Inst. Meth. A **554**, 147 (2005).
2. S. Nussinov, R. D. Peccei, X. M. Zhang, Phys.Rev. D **63**, 016003 (2000);
3. W. J. Huo, C. X. Yue, T. F. Heng, Phys.Rev. D **67**, 114001 (2003);
4. Z. Silagadze, Phys. Scripta **64**, 128 (2001) ;
5. M.A. Sanchis-Lozano, Int. J. Mod. Phys. A **19**, 2183 (2004); hep-ph/0307313.
6. CLEO Collaboration, J.L. Rosner *et al.*, Phys. Rev. Lett. **96**, 092003 (2006).
7. CLEO Collaboration, G. Adams *et al.*, Phys. Rev. Lett. **94**, 012001 (2005).
8. CLEO Collaboration, Y. Kubota *et al.*, Nucl. Inst. Meth. A **320**, 66 (1992); D. Bortoletto *et al.*, Nucl. Inst. Meth. A **320**, 114 (1992).
9. R. Kleiss and S. van der Marck, Nucl. Phys. B **342**, 61 (1990).
10. C.M. Carloni Calame *et al.*, Nucl. Phys. Proc. Suppl. B **131**, 48 (2004).
11. S. Jadach and Z. Was, Acta Phys. Polon. B **15**, 1151 (1984); Erratum - *ibid.* B **16**, 483 (1985); S. Jadach and Z. Was, Comput. Phys. Commun. **36**, 191 (1985); *ibid.* **64**, 267 (1990); *ibid.* **85**, 453 (1995).
12. S. Jadach, J. H. Kuhn, and Z. Was, Comput. Phys. Commun. **64**, 275 (1990); M. Jezabek, Z. Was, S. Jadach, and J. H. Kuhn, *ibid.* **70**, 69 (1992); S. Jadach, Z. Was, *ibid.* **76**, 361 (1993); R. Decker, E. Mirkes, R. Sauer, and Z. Was, Z. Phys. C **58**, 445 (1993).
13. E. Barberio, B. van Eijk and Z. Was, Comput. Phys. Commun. **66**, 115 (1991); E. Barberio and Z. Was, Comput. Phys. Commun. **79**, 291 (1994).
14. R. Brun *et al.*, GEANT 3.21, CERN Program Library Long Writeup W5013 (1993).
15. T. Sjöstrand *et al.*, Computer Physics Commun. **135**, 238 (2001).
16. QQ - The CLEO Event Generator, http://www.lns.cornell.edu/public/CLEO/soft/QQ.
17. S. Godfrey and J.L. Rosner, Phys.Rev. D **64**, 074011 (2001); Erratum - *ibid.* D **65**, 039901 (2002).
18. Particle Data Group, S. Eidelman *et al.*, Phys. Lett. B, **1** (2004).